Coupled-mode theory for film-coupled plasmonic nanocubes

Patrick T. Bowen* and David R. Smith†

Center for Metamaterials and Integrated Plasmonics and Department of Electrical and Computer Engineering, Duke University, P.O. Box 90291, Durham, North Carolina 27708, USA

(Received 3 July 2014; revised manuscript received 13 October 2014; published 3 November 2014)

Planar metallic nanoparticles separated by nanoscale distances from a metal film support unique plasmonic resonances useful for controlling a wide range of photodynamic processes. The fundamental resonance of a film-coupled planar nanoparticle arises from a transmission-line mode localized between nanoparticle and film, whose properties can be roughly approximated by closed form expressions similar to those used in patch antenna theory. The insight provided by the analytical expressions, and the potential of achieving similar closed-form expressions for a range of plasmonic phenomenon such as spasing, fluorescence enhancement, and perfect absorbers, motivates a more detailed study of the film-coupled patch. Here, we present an expanded analytical analysis of the plasmonic patch geometry, applying an eigenmode expansion method to arrive at a more accurate description of the field distribution underneath a film-coupled plasmonic nanocube. The fields corresponding to the inhomogeneous Maxwell's equations are expanded in a set of lossless waveguide eigenmodes. Radiation damping and Ohmic losses are then perturbatively taken into account by considering an equivalent surface impedance. We find that radiative loss couples the lossless eigenmodes, leading to discernible features in the scattering spectra of the nanocubes. The method presented can be further applied to the case of point source excitations, in which accounting for all potential eigenmodes becomes essential.

DOI: 10.1103/PhysRevB.90.195402 PACS number(s): 42.25.Bs

I. INTRODUCTION

The use of plasmonic nanostructures for enhancing photodynamic processes in nearby emitters has been well documented. An emitter placed within the gap of two closely separated nanoparticles, or near a sharp corner or tips of a nanoparticle, experiences a strongly modified electromagnetic environment, with large optical field enhancements and an enhanced radiative density of states [1–3]. A wide variety of optical phenomena can be impacted within such enhancement volumes, including fluorescence [4], photocatalysis [5], optical bistability [6], surface plasmon amplification (spasing) [7], two-photon absorption [8], four-wave mixing [9], and many others.

Film-coupled plasmonic nanocubes and other planar film-coupled systems represent advantageous plasmonic platforms for several reasons. The field distribution of a nanoparticle spaced closely above a metal film strongly resembles that of a nanoparticle dimer [10]—two nanoparticles separated by a nanoscale gap—which is known to exhibit some of the largest and most strongly localized field enhancements [11]. The film-coupled nanoparticle system retains the desirable field enhancement properties of the dimer; however, film-coupled nanoparticle systems are much more controllable and amenable to experimental realization, particularly for the most extreme (subnanometer) gap dimensions [12]. The film-coupled geometry as an experimental platform has allowed nearly unprecedented control over the gap thickness, leveraging planar deposition methods such as layer-by-layer approaches for organic spacer layers, or atomic layer deposition (ALD) for inorganic spacer layers.

Distinct from nanosphere dimers or even film-coupled nanospheres, film-coupled planar nanoparticles, such as nanocubes or nanoplatelets, possess a rich mode structure that can easily be controlled in experiment. Film-coupled planar nanoparticles support gap-plasmon modes, characterized by fields that are confined and propagate between the nanoparticle and film [13–15]. The gap-plasmon modes can be understood from transmission line theory, modified suitably by taking into account the dispersion of the metal.

While any film-coupled planar nanoparticle or nanoplatelet will support the distinctive transmission line gap plasmons, here we are motivated by recent experimental studies to consider nanocubes as a concrete conceptual implementation. Nanocubes can be fabricated by colloidal methods and readily deposited on an insulating spacer layer over a metal film. Film-coupled nanocubes were suggested as a convenient and inexpensive means of forming large-area, controlled reflectance surfaces [16], and have more recently been applied in the context of fluorescence enhancement [4]. The scattering properties of a film-coupled nanocube at optical wavelengths bear considerable resemblance to those of the patch antenna, ubiquitous in microwave engineering. Methods of analysis to predict the radiation characteristics of driven patch antennas are well known in microwave engineering and are becoming increasingly common to describe the scattering characteristics of optical patch antennas. The film-coupled nanocube can be considered as an example of an optical patch antenna, though we note the theoretical approach outlined here is not restricted to nanocubes.

Ciraci *et al.* [14] recently presented an analytical treatment of the scattering characteristics of a film-coupled nanocube, applying the transmission line circuit model to solve for the gap-plasmon propagating in the gap between the cube and film. The nanocube was assumed to be excited to a normally incident plane wave, coupled to the nanocube resonance via the magnetic flux passing through the gap. The transmission

*patrick.bowen@duke.edu
†drsmith@ee.duke.edu

line model for the nanopatch antenna was modified by introducing the gap-plasmon dispersion relation, allowing the more complex optical response of the metal to be modeled. In this work, only the fundamental cavity mode of the nanopatch was considered. A comparison of the resulting analytical formulas with full-wave numerical simulations revealed reasonable agreement between the spectral properties of the nanopatch as well as the field enhancement within the gap region as a function of excitation wavelength; however, additional mode structure found in the numerical simulations, as well as in later experiments [17], was not captured by the analytical treatment and was presumed to be related to higher-order mode excitation.

Our goal in the present paper is to use coupled-mode theory (CMT) [18–23] to provide a more detailed analytical analysis of the film-coupled nanocube system that incorporates potentially all of the higher order modes that can be excited within the gap region. The complete mode set assumes greater importance, for example, when the excitation is a point source located within the gap region. By including all higher order modes, we effectively construct the Green's function for the nanopatch, which can ultimately be used to determine the optical properties of emitters embedded within the gap region.

The model presented in this paper is not unlike the cavity model used for patch antennas [24], where the gap between the patch and the metal film is modeled as a resonator cavity with perfectly electric conducting (PEC) boundaries on the patch and ground plane surfaces and perfectly magnetic conducting (PMC) boundaries on the gaps. In this paper, we develop a similar model for the film-coupled nanocube system, but modify it by analytically including the coupling to the incident field, gap plasmon effects, and the Ohmic and radiative losses.

We begin by introducing the standard cavity eigenmode expansion of Maxwell's equations [25], derived using a variation of Lorenz reciprocity. We then define an eigenvalue problem that is similar to the real problem but excluding all lossless by replacing the gap volume with a lossless, rectangular cavity, where the open slots replaced by PMCs and the dielectric constant of the metal is purely real. The field solutions within the lossless cavity can be expressed as a set of orthogonal eigenmodes, which we define as the lossless eigenmodes. We take this approximation initially as an *ansatz*, later confirming its validity by full-wave simulation. The coupling of the incident field to the eigenmodes and the radiative losses can then be found analytically using the lossless eigenmode fields. Ohmic losses are found by allowing the imaginary part of the dielectric constant to resume its physical value and integrating the resulting Poynting vector over the metal surfaces.

When losses are included in any system, the eigenvalues are no longer real and the eigenmodes are no longer necessarily orthogonal. This has been recently demonstrated specifically for plasmonic resonances by Lalanne *et al.* [21], where it was shown that mode nonorthogonality must be taken into account in order to compute the correct eigenmode amplitude spectrum. In this paper the eigenmode nonorthogonality is handled in three different approaches. In the first approach, mode nonorthogonality is ignored and all of the modes are assumed to be decoupled. Assuming that the modes are orthogonal allows very intuitive and simple equations to be derived that describe the resonances of the gap plasmon eigenmodes.

In the second approach, the losses and the resulting eigenmode cross coupling is calculated based on the assumption of a surface impedance of the slots. The surface-impedance approach is able to explain the presence of resonances in the amplitude spectrum that are observed in simulation, but should be zero if the modes are orthogonal. Some of these resonances can be considered "dark" in the sense that they cannot directly couple to the far field, but are excited by cross coupling with a bright mode.

The third and final approach presented utilizes a Fourier method [24] to calculate the radiation damping and cross coupling between modes. This approach results in the best match between the analytically computed eigenmode amplitude spectrum and the amplitude spectrum extracted from simulation.

II. DERIVATION OF EIGENMODE COUPLED EQUATIONS

Our goal in this section is to solve for the fields within the gap region of a film-coupled nanocube, assuming excitation by an incident driving wave. We assume the actual electric and magnetic fields within the gap can be expanded in a sum over cavity eigenmodes, defined by the volume underneath the nanocube as well as the bounding metal and free-space surfaces, or

$$\mathbf{E} = \sum_{\mu} e_{\mu}(\omega)\mathbf{E}_{\mu}(\mathbf{r}) \tag{1a}$$

$$\mathbf{H} = \sum_{\mu} h_{\mu}(\omega)\mathbf{H}_{\mu}(\mathbf{r}). \tag{1b}$$

We seek to determine the electric and magnetic field coefficients and their dependence on the driving field, radiation damping, and Ohmic losses. In the following, we derive a set of two coupled infinite-rank matrix equations: one in which radiative damping appears as a perturbative term and another in which Ohmic loss appears as a perturbative term. The perturbative terms additionally serve to couple the eigenmodes together.

Each of the eigenmodes satisfies the homogeneous Maxwell's equations, or

$$\nabla \times \mathbf{H}_{\mu} = j\omega_{\mu}\epsilon_0\mathbf{E}_{\mu} \tag{2a}$$

$$\nabla \times \mathbf{E}_{\mu} = -j\omega_{\mu}\mu_0\mathbf{H}_{\mu}. \tag{2b}$$

As a starting point, we first assume the fields can be expanded in the set of lossless eigenmodes. To obtain lossless eigenmodes, we replace the slots by PMCs and requiring the dielectric constant of the metal film to be real, as shown in Fig. 1(b). Simulation results and previous work show that modes in which the electric field is zero on the boundaries are overly damped and do not play a role in the system response. Thus, for the modes of relevance, the electric field is maximum and the magnetic field is minimum at the slots (or gap edges) of the cube.

The eigenvalue problem given by Eqs. (6a) and (6b), together with the PMC and metal boundary conditions, is

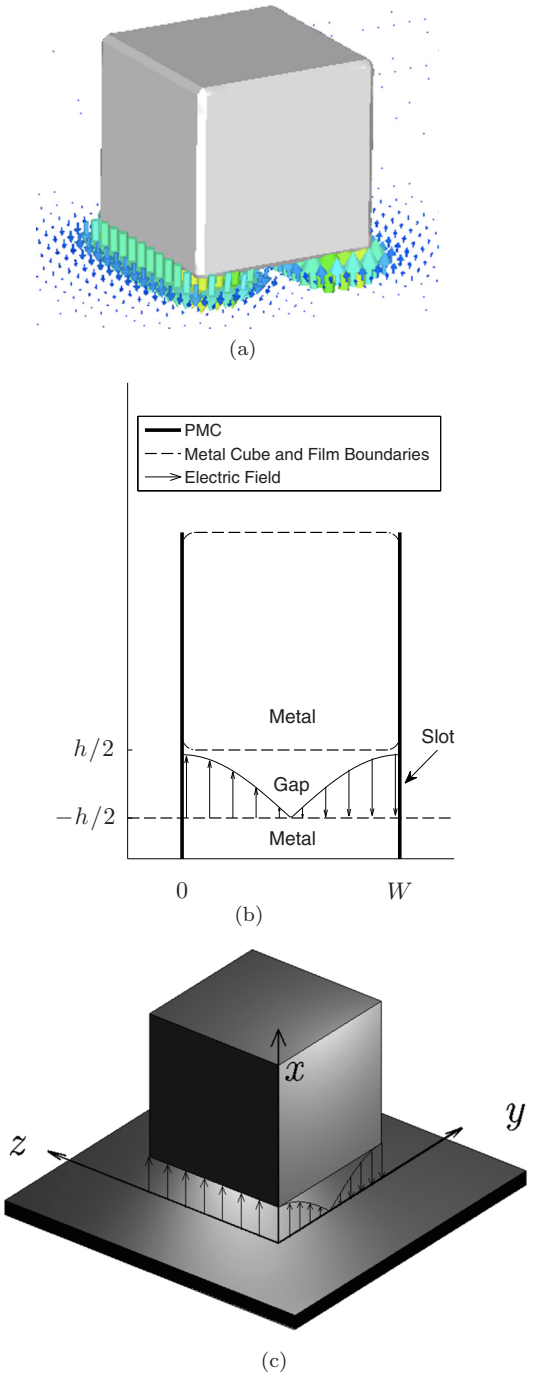

FIG. 1. (Color online) (a) Fields from a simulated film-coupled nanocube at the resonance frequency of the $\mathbf{E}_{01}$ mode. (b) The lossless cavity eigenmode problem, with boundary conditions. (c) Illustration of coordinate system convention for a film-coupled nanocube.

satisfied if (see Fig. 2) [24]

$$E^x_{mn} = E_0 \cos(k_{xmn}x)\cos(m\pi y/W)\cos(n\pi z/W) \quad (3a)$$

$$E^y_{mn} = E_0 \frac{k_{xmn}W}{\pi}\frac{m}{m^2+n^2}\sin(k_{xmn}x)\sin(m\pi y/W) \times \cos(n\pi z/W) \quad (3b)$$

$$E^z_{mn} = E_0 \frac{k_{xmn}W}{\pi}\frac{n}{m^2+n^2}\sin(k_{xmn}x) \times \cos(m\pi y/W)\sin(n\pi z/W) \quad (3c)$$

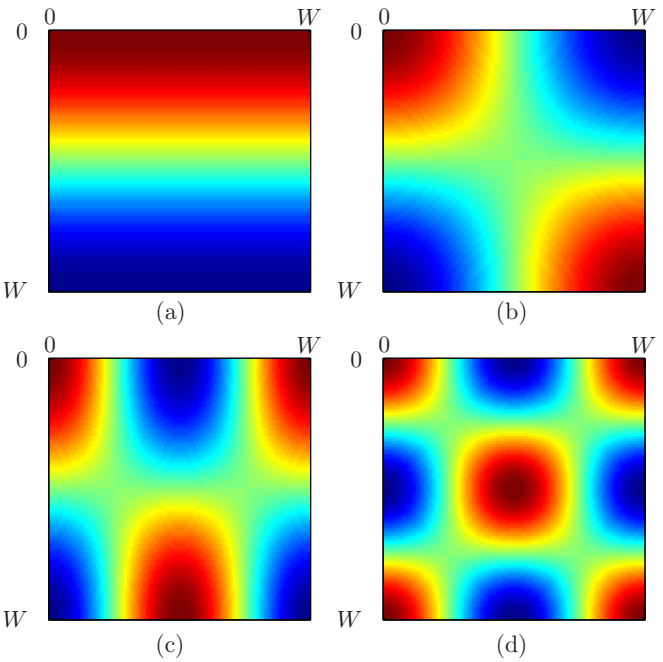

FIG. 2. (Color online) The lossless eigenmodes (a) $\mathbf{E}_{0,1}(\mathbf{r})$, (b) $\mathbf{E}_{1,1}(\mathbf{r})$, (c) $\mathbf{E}_{2,1}(\mathbf{r})$, and (d) $\mathbf{E}_{2,2}(\mathbf{r})$.

$$H^x_{mn} = 0 \quad (3d)$$

$$H^y_{mn} = -i\frac{E_0}{Z_0}\frac{\omega_{mn}W}{c\pi}\frac{n}{m^2+n^2} \times \cos(k_{xmn}x)\cos(m\pi y/W)\sin(n\pi z/W) \quad (3e)$$

$$H^z_{mn} = i\frac{E_0}{Z_0}\frac{\omega_{mn}W}{c\pi}\frac{m}{m^2+n^2} \times \cos(k_{xmn}x)\sin(m\pi y/W)\cos(n\pi z/W) \quad (3f)$$

for $(x,y,z) \in V$, where V is the volume of the gap: $V = \{[-h/2,h/2] \times [0,W] \times [0,W]\}$. In these equations, ω_{mn} is the resonance frequency, $Z_0 = \sqrt{\frac{\mu_0}{\epsilon_0}}$ is the impedance of free space, c is the speed of light, and E_0 is an arbitrary constant with units of electric field that is used to normalize the modes. The double index mn was used in these equations rather than the single index μ to classify the modes in terms of the number of nodes in the y and z directions.

Unlike patch antennas, where the metal is considered to be PEC, k_{xmn} must be allowed to be nonzero and the plasmon dispersion relation must be used to find k_{xmn} and ω_{mn}. In the metal, the fields follow the same y,z dependence as Eq. (3), but with an exponential decay of $e^{-\kappa_{mn}|x|}$ into the metal. The plasmon dispersion relation for an infinite parallel plate metal-insulator-metal waveguide, together with the Helmholtz equation evaluated in the gap and in the metal, provide three equations that can be simultaneously solved for three unknowns $\{k_{xmn},\kappa_{mn},\omega_{mn}\}$:

$$\tan\left(\frac{k_{xmn}h}{2}\right) + \frac{j\kappa_{mn}}{k_{xmn}\mathrm{Re}\{\epsilon(\omega_{mn})\}} = 0 \quad (4a)$$

$$\left(\frac{m\pi}{W}\right)^2 + \left(\frac{n\pi}{W}\right)^2 + k^2_{xmn} = \frac{\omega^2_{mn}}{c^2} \quad (4b)$$

$$\left(\frac{m\pi}{W}\right)^2+\left(\frac{n\pi}{W}\right)^2-\kappa_{mn}^2=\mathrm{Re}\{\epsilon(\omega_{mn})\}\frac{\omega_{mn}^2}{c^2}, \quad (4c)$$

where the real part of the permittivity was used to keep the modes lossless. If the permittivity is real then k_{xmn} must be purely imaginary, as has been shown in previous work developing a transmission line model for nanocube resonances [14].

The modes introduced in Eq. (3) are lossless and orthogonal, and their orthogonality makes them a convenient basis to use when expanding the field in the gap. However, the expansion in terms of Eq. (3) would not allow the losses of the real nanocube system to be taken into account. Therefore we will also need an expansion in terms of lossy eigenmodes,

$$\mathbf{E}=\sum_\mu \tilde{e}_\mu(\omega)\tilde{\mathbf{E}}_\mu(\mathbf{r}) \quad (5a)$$

$$\mathbf{H}=\sum_\mu \tilde{h}_\mu(\omega)\tilde{\mathbf{H}}_\mu(\mathbf{r}), \quad (5b)$$

which are defined by the source-free solution to Maxwell's equations in the exact nanocube geometry,

$$\nabla\times\tilde{\mathbf{H}}_\mu=j\tilde{\omega}_\mu\epsilon(\mathbf{r},\tilde{\omega}_\mu)\tilde{\mathbf{E}}_\mu \quad (6a)$$

$$\nabla\times\tilde{\mathbf{E}}_\mu=-j\tilde{\omega}_\mu\mu_0\tilde{\mathbf{H}}_\mu, \quad (6b)$$

including the full complex permittivity and radiative boundary conditions on the slots. Although the exact solution to this eigenvalue problem is unknown, the solution inside the gap and sufficiently far from the slots must converge to Eqs. (3) and (4), with the exception that the complex permittivity must be used in Eq. (4).

Using the lossless eigenmode expansion of the fields, we seek to solve the inhomogeneous Maxwell's equations, or

$$\nabla\times\mathbf{H}=j\omega\epsilon_0\mathbf{E}+\mathbf{J}_e \quad (7a)$$

$$\nabla\times\mathbf{E}=-j\omega\mu_0\mathbf{H}-\mathbf{J}_m. \quad (7b)$$

The arbitrary field distribution can be expanded into a sum of lossless eigenmodes as in Eqs. (5a) and (5b), where the mode amplitudes and fields are indexed with the single variable μ rather than the pair mn for convenience, but without loss of generality. Note that the mode amplitudes are functions of frequency. We take the inner product of the electric curl equation with $\mathbf{E}_\mu^*$:

$$\int\mathbf{E}_\mu^*\cdot(\nabla\times\mathbf{H})dV=j\omega\epsilon_0\int\mathbf{E}_\mu^*\cdot\mathbf{E}dV+\int\mathbf{E}_\mu^*\cdot\mathbf{J}_e dV. \quad (8)$$

Using standard vector identities and substitution of the homogeneous Maxwell's equations given in Eqs. (6a) and (6b), we obtain

$$\mathbf{E}_\mu^*\cdot(\nabla\times\mathbf{H})=\mathbf{H}\cdot(\nabla\times\mathbf{E}_\mu^*)-\nabla\cdot(\mathbf{E}_\mu^*\times\mathbf{H}) \quad (9)$$

$$=j\omega_\mu\mu_0\mathbf{H}\cdot\mathbf{H}_\mu^*-\nabla\cdot(\mathbf{E}_\mu^*\times\mathbf{H}). \quad (10)$$

Substituting these equations, we obtain

$$j\omega_\mu\mu_0\int\mathbf{H}\cdot\mathbf{H}_\mu^*dV-\int(\mathbf{E}_\mu^*\times\mathbf{H})\cdot\mathbf{n}dS=j\omega\epsilon_0\int\mathbf{E}_\mu^*\cdot\mathbf{E}dV+\int\mathbf{E}_\mu^*\cdot\mathbf{J}_e dV, \quad (11)$$

where the surface integral is evaluated over the boundary of the gap region V, and $\mathbf{n}$ is the normal vector to the surface. Using the orthogonality of the lossless eigenmodes and substituting Eqs. 5(a) and 5(b), the equation simplifies to

$$j\omega e_\mu-j\omega_\mu h_\mu+\frac{1}{2U_\mu}\int(\mathbf{E}_\mu^*\times\mathbf{H})\cdot\mathbf{n}dS=-\frac{1}{2U_\mu}\int\mathbf{E}_\mu^*\cdot\mathbf{J}_e dV, \quad (12)$$

where

$$U_\mu=\frac{\epsilon_0}{2}\int|\mathbf{E}_\mu|^2dV=\frac{\mu_0}{2}\int|\mathbf{H}_\mu|^2dV \quad (13)$$

are the normalization constants for the electric and magnetic energy in the cavity, respectively. The uniqueness theorem ensures that the electric and magnetic field energies are equal for the lossless eigenmodes [25].

Although we have used the lossless magnetic eigenmodes to reduce the first volume integral in Eq. (11), we have not reduced the surface integral term in the same manner, as it requires more care. Because the boundary conditions on the fields at the slots are open rather than PMC, the tangential component of the magnetic field at the slots is not precisely zero, as is the case for the lossless eigenmodes in Eq. (3). Therefore, a field expansion on the slot surface in terms of the lossless magnetic modes $\mathbf{H}_\mu$ cannot be performed since this expansion could never reproduce the appropriate radiation boundary condition. Instead, we expand the field on the surface in terms of lossy modes, $\mathbf{H}=\sum_\nu\tilde{h}_\nu\tilde{\mathbf{H}}_\nu$. Then the surface integral in Eq. (12) can be expressed as

$$\frac{1}{2U_\mu}\int(\mathbf{E}_\mu^*\times\mathbf{H})\cdot\mathbf{n}dS=\sum_\nu\frac{\tilde{h}_\nu(\omega)}{2U_\mu}\int(\mathbf{E}_\mu^*\times\tilde{\mathbf{H}}_\nu)\cdot\mathbf{n}dS=\sum_\nu\tilde{h}_\nu(\omega)P_{\mu\nu}^{\mathrm{rad}}. \quad (14)$$

The matrix $P_{\mu\nu}^{\mathrm{rad}}=\int(\mathbf{E}_\mu^*\times\tilde{\mathbf{H}}_\nu)\cdot\mathbf{n}dS/2U_\mu$ is representative of losses, but is normalized by the mode energy to have units of frequency. It includes a contribution from both Ohmic losses and radiative losses, with Ohmic losses resulting when the integral is evaluated on the metal surfaces and radiative losses when it is evaluated on the slots. However, the Ohmic loss contribution in this integral is vanishing when $k_{x\mu}h/2$ is small and can be neglected when the gap size is small. Therefore we use this matrix to include only the radiative losses by evaluating the surface integral only over the slots. The main contribution to Ohmic losses will be included later by considering the analogous equation derived from the electric curl equation.

Even though the magnetic fields of the lossy eigenmodes are unknown in the slots, if the total tangential electric field on the edge of the cube is well approximated by a sum of the electric fields of the lossless eigenmode fields, then

a Fourier transform method can be used to solve for the magnetic field in the slot due to the electric field from each eigenmode. In this method, the lossy eigenmode magnetic field is approximated in the slots by the magnetic field that must exist in each slot given the radiative boundary condition and the existence of an electric field $\mathbf{E}_\nu$ in the gap, where $\mathbf{E}_\nu$ is the electric field from the lossless eigenmode. The method is outlined in Appendix B, where coefficients of the form $\frac{1}{2}\int(\mathbf{E}_\mu^* \times \tilde{\mathbf{H}}_\nu)\cdot\mathbf{n}dS$ are evaluated based on the expression for $\tilde{\mathbf{E}}_\mu$ given by the lossless eigenmode problem. The fundamental resonance of the film-coupled nanocube radiates particularly strongly, and so the radiative losses must be taken into account [26] despite the deeply subwavelength scale of the structure [27].

We note that the surface integral in Eq. (14) is also representative of the extent to which mode orthogonality has been broken by the existence of losses. The diagonal elements of $P_{\mu\nu}^{\mathrm{rad}}$ represent the losses of the individual eigenmodes, and the off-diagonal elements will be shown later to function as a cross coupling between the modes.

This expansion, left as it is, remains unuseful because the introduction of the coefficients $\tilde{h}_\mu$ will yield more variables than equations. However, if the losses included in the lossy eigenvalue problem are sufficiently small, then $\mathbf{H}_\mu \approx \tilde{\mathbf{H}}_\mu$ in the volume of the gap. In this case, the expansion of the field into lossless and lossy eigenmodes will yield approximately the same coefficients, so that $h_\mu \approx \tilde{h}_\mu$. Applying that approximation yields the first of two coupled equations needed to solve the system:

$$j\omega e_\mu - j\omega_\mu h_\mu + \sum_\nu h_\nu(\omega)P_{\mu\nu}^{\mathrm{rad}} = -\frac{1}{2U_\mu}\int \mathbf{E}_\mu^*\cdot\mathbf{J}_e dV. \tag{15}$$

The second equation for the electric and magnetic coefficients can be derived using the curl equation for the electric field and following a similar procedure:

$$j\omega h_\mu - j\omega_\mu e_\mu + \frac{1}{2U_\mu}\int(\mathbf{E}\times\mathbf{H}_\mu^*)\cdot\mathbf{n}dS = -\frac{1}{2U_\mu}\int \mathbf{H}_\mu^*\cdot\mathbf{J}_m dV. \tag{16}$$

To derive this equation, both sides of the curl equation were multiplied by the mode magnetic field $\mathbf{H}_\mu$, and then mode orthogonality was applied. The electric field in the surface integral can be expanded into a sum of lossy eigenmodes, $\mathbf{E} = \sum_\nu \tilde{e}_\nu\tilde{\mathbf{E}}_\nu \approx \sum_\nu e_\nu\tilde{\mathbf{E}}_\nu$, that satisfy the boundary conditions of the lossy metal film

$$j\omega h_\mu - j\omega_\mu e_\mu + \sum_\nu e_\nu\frac{1}{2U_\mu}\int(\tilde{\mathbf{E}}_\nu\times\mathbf{H}_\mu^*)\cdot\mathbf{n}dS = -\frac{1}{2U_\mu}\int \mathbf{H}_\mu^*\cdot\mathbf{J}_m dV. \tag{17}$$

The lossless eigenmode field $\mathbf{H}_\mu^*$ has zero tangential component on the surfaces of the slot, and therefore the surface integral vanishes on the edges of the cube and doesn't contribute to radiative loss. It does not, however, vanish on the metal surface, so Ohmic losses may be included in this surface integral:

$$j\omega h_\mu - j\omega_\mu e_\mu + \sum_\nu e_\nu(\omega)P_{\mu\nu}^{\Omega} = -\frac{1}{2U_\mu}\int \mathbf{H}_\mu^*\cdot\mathbf{J}_m dV \tag{18}$$

$$P_{\mu\nu}^{\Omega} = \frac{1}{2U_\mu}\int(\tilde{\mathbf{E}}_\nu\times\mathbf{H}_\mu^*)\cdot\mathbf{n}dS. \tag{19}$$

A detailed evaluation of the Ohmic losses is given in Appendix A. It is also shown that the Ohmic loss matrix is zero for the film-coupled nanocube system if $\mu \neq \nu$, so Eq. (18) can be further simplified as

$$j\omega h_\mu - \left(j\omega_\mu - P_\mu^{\Omega}\right)e_\mu = -\frac{1}{2U_\mu}\int \mathbf{H}_\mu^*\cdot\mathbf{J}_m dV. \tag{20}$$

Equations (15) and (20) form a set of linear equations that can be solved for the coefficients $\{e_\mu(\omega),h_\mu(\omega)\}$.

Note that a simpler, alternative formulation to evaluating the far-field coupling in Eq. (12) may be found by assuming a gap admittance so that, at every point along the edge of the cube, we have that

$$\mathbf{H}_t = Y_g\mathbf{E}\times\mathbf{n}. \tag{21}$$

If Eq. (21) is used in Eq. (15), then the boundary term becomes a sum over electric field coefficients instead of magnetic field coefficients. The equivalent matrix equation becomes

$$j\omega e_\mu - j\omega_\mu h_\mu + \sum_\nu e_\nu P_{\mu\nu}^{\mathrm{rad}} = -\frac{1}{2U_\mu}\int \mathbf{E}_\mu^*\cdot\mathbf{J}_e dV, \tag{22}$$

where the surface integral becomes a surface overlap integral of the tangential electric fields:

$$P_{\mu\nu}^{\mathrm{rad}} = \frac{Y_g}{2U_\mu}\int(\mathbf{E}_\mu^*\times\mathbf{n})\cdot(\mathbf{E}_\nu\times\mathbf{n})dS. \tag{23}$$

Depending on the frequency dependence of the gap admittance, this system will behave slightly differently as a function of frequency than Eq. (15), since the radiative losses are now coupled through the electric eigenmode amplitudes rather than the magnetic eigenmode amplitudes.

III. COUPLING TO THE FAR-FIELD

Equations (15) and (16) include source terms that relate to electric currents [Eq. (14)] and effective magnetic currents [Eq. (18)]. To investigate the scattering from the film-coupled nanocube illuminated by an external driving field, $(\mathbf{E}_0,\mathbf{H}_0)$, our strategy is to compute the effective source terms based on the application of one of Schelkunoff's equivalence principles [24,25,28]. Consider the surface defined by the eigenmode problem, but excluding the PMC at the slots. The total electric and magnetic fields inside this surface can be found through the scattering of an equivalent electric and an equivalent magnetic surface current, which are given by the tangential magnetic and electric fields at the slot, respectively. The electric and magnetic surface currents are given by

$$\mathbf{K}_e = \mathbf{n}\times\mathbf{H} \qquad \mathbf{r}\in\partial V \tag{24a}$$

$$\mathbf{K}_m = \mathbf{E}\times\mathbf{n} \qquad \mathbf{r}\in\partial V, \tag{24b}$$

where $\mathbf{H}$ and $\mathbf{E}$ are the total tangential electric and magnetic fields, including both the incident and scattered fields. The coupling of the incident electric and magnetic fields into a particular eigenmode is given by

$$\int \mathbf{E}_\mu^* \cdot \mathbf{J}_e dV = \int \mathbf{E}_\mu^* \cdot \mathbf{K}_e dS = -\int (\mathbf{E}_\mu^* \times \mathbf{H}) \cdot \mathbf{n} dS \quad (25a)$$

$$\int \mathbf{H}_\mu^* \cdot \mathbf{J}_m dV = \int \mathbf{H}_\mu^* \cdot \mathbf{K}_m dS = -\int (\mathbf{E} \times \mathbf{H}_\mu^*) \cdot \mathbf{n} dS. \quad (25b)$$

We seek to evaluate these expressions for the special case where the system is excited by a plane wave at normal incidence, and in the long-wavelength limit where the incident field $\{\mathbf{E}_0, \mathbf{H}_0\}$ can be considered a constant vector field over the film-coupled nanocube system.

The electric current coupling in Eq. (25a) must be zero on the metal surfaces, since the overlap integral of the tangential part of the lossless modes with a normally incident plane wave is zero on those surfaces. On the slots, the mode's lossless magnetic field is zero, and so the total magnetic field on the slot is approximated by the incident magnetic field. The incident magnetic field is symmetric, while the normal vector to any two opposing slots is asymmetric. Therefore the incident magnetic field can only couple to modes that are asymmetric in the electric field.

The magnetic current coupling must likewise be zero in the slots, where the lossless mode's tangential magnetic field is zero. On the bottom of the cube and the top of the film, the electric field of the lossless eigenmode is symmetric, and the incident electric field is also very nearly symmetric on the bottom of the cube and top of the metal film when applied at normal incidence. Therefore the total incident and scattered field will be very nearly symmetric on the two metal surfaces. Since the electric field is symmetric, the mode's magnetic field is symmetric, and the normal vector is asymmetric, the equivalent magnetic current (and hence the incident electric field) does not couple to the cube system at normal incidence. Then the coupling into the modes reduces to

$$\int \mathbf{E}_\mu^* \cdot \mathbf{J}_e dV = -2 \int_{\text{slots}} (\mathbf{E}_\mu^* \times \mathbf{H}_0) \cdot \mathbf{n} dS \quad (26)$$

$$\int \mathbf{H}_\mu^* \cdot \mathbf{J}_m dV = 0, \quad (27)$$

where $\mathbf{H}_0$ is the incident magnetic field, and the additional factor of two is due to the reflection of the incident field off of the metal film [24].

IV. RESULTS

A. No modal cross-coupling approximation

If the radiative loss rate matrix $P_{\mu\nu}^{\text{rad}}$ is diagonal, then the two equations for the electric and magnetic field present a coupled system of oscillators:

$$j\omega e_\mu - \left(j\omega_\mu - P_\mu^{\text{rad}}\right) h_\mu = -\frac{1}{2U_\mu} \int \mathbf{E}_\mu \cdot \mathbf{J}_e dV \quad (28)$$

$$j\omega h_\mu - \left(j\omega_\mu - P_\mu^{\Omega}\right) e_\mu = -\frac{1}{2U_\mu} \int \mathbf{H}_\mu \cdot \mathbf{J}_m dV. \quad (29)$$

We can immediately gain insight into the mechanism of the interaction between elements in the system from the equations of motion above. The magnetic field and electric field are coupled to one another through the constant coupling coefficients of $j\omega_\mu$. The electric current drives the electric mode, while the magnetic current drives the magnetic mode. Because of the way in which the lossy eigenmodes were introduced, energy in the form of radiative losses exits the system through the magnetic field, and ohmic losses exit the system through the electric field. The solution to the coupled system is

$$e_\mu = \frac{-j\omega \frac{1}{2U_\mu} \int \mathbf{E}_\mu^* \cdot \mathbf{J}_e dV - \left(j\omega_\mu - P_\mu^{\text{rad}}\right) \frac{1}{2U_\mu} \int \mathbf{H}_\mu^* \cdot \mathbf{J}_m dV}{\left(j\omega_\mu - P_\mu^{\text{rad}}\right)\left(j\omega_\mu - P_\mu^{\Omega}\right) + \omega^2} \quad (30)$$

$$h_\mu = \frac{-\left(j\omega_\mu - P_\mu^{\Omega}\right) \frac{1}{2U_\mu} \int \mathbf{E}_\mu^* \cdot \mathbf{J}_e dV - j\omega \frac{1}{2U_\mu} \int \mathbf{H}_\mu^* \cdot \mathbf{J}_m dV}{\left(j\omega_\mu - P_\mu^{\text{rad}}\right)\left(j\omega_\mu - P_\mu^{\Omega}\right) + \omega^2}. \quad (31)$$

The system can be simplified by applying the coupling coefficients for the incident field:

$$e_\mu = \frac{j\omega \int (\mathbf{E}_\mu^* \times \mathbf{H}_0) \cdot \mathbf{n} dS / U_\mu}{\left(j\omega_\mu - P_\mu^{\text{rad}}\right)\left(j\omega_\mu - P_\mu^{\Omega}\right) + \omega^2} \quad (32a)$$

$$h_\mu = \left(\omega_\mu/\omega - j P_\mu^{\Omega}/\omega\right) e_\mu. \quad (32b)$$

If the fundamental mode, $(m,n) = (1,0)$, is assumed to be the only important mode within the frequency range of interest and $k_{x\mu} h/2$ is sufficiently small, then Eq. (32a) leads to a very simple expression for the enhancement factor near the fundamental resonance:

$$\mathbf{E}(\mathbf{r},\omega)/E_0 = e_{1,0}(\omega) \mathbf{E}_{1,0}(\mathbf{r}) \quad (33)$$

$$\approx \frac{(j8\omega c/W)\cos(\pi y/W)}{\omega^2 - \omega_{1,0}^2 - j\omega_{1,0}\left(P_{1,0}^{\text{rad}} + P_{1,0}^{\Omega}\right) + P_{1,0}^{\Omega} P_{1,0}^{\text{rad}}} \quad (34)$$

$$\approx \frac{(j8\omega c/W)\cos(\pi y/W)}{\omega^2 - \omega_{1,0}^2 - j\omega_{1,0}\left(P_{1,0}^{\text{rad}} + P_{1,0}^{\Omega}\right)}. \quad (35)$$

Hence, the imaginary part of the slot impedance functions as a frequency shift of the mode, and the real part contributes to losses. Similar equations to Eq. (35) can be easily derived for all of the higher order modes.

The primary difficulty from here is in determining the imaginary part of the radiative loss. The electric field is very uniform across the slots, and for the lowest order mode it is also constant along one of the dimensions of the cube. This suggests that the impedance for an infinitely wide slot with a constant field could be used [24]:

$$Y_g = \frac{hk}{2}(1 - (kh)^2/24 + j[1 - 0.636 \ln(kh)]), \quad (36)$$

where $k = \omega/c$. The real part of the radiative loss can be accurately fixed using the radiation resistance from patch antenna theory. The radiation resistance $R_r(\omega)$ for the fundamental mode is well known and is given in many textbooks [14,24].

The radiated power can then be written as

$$P_{1,0}^{\text{rad}} = \frac{h^2 E_0^2}{2R_r(\omega)} + j\frac{\text{Im}\{Y_g\}}{2}\int |\mathbf{n}\times\mathbf{E}_{1,0}|^2 dS. \quad (37)$$

The above analytical equations were tested against full-wave FEM simulations in CST Microwave Studio of a nanocube of dimension 80 nm and separated 5 nm air gap from the metal substrate. The nanocube and metal film were composed of silver using data from Johnson and Christy [29]. The edges of the nanocube were given a radius of curvature of 3 nm to accommodate the tetrahedral mesh. A mode amplitude spectrum was extracted from the electric fields obtained from the simulation by taking the overlap integral of the simulated fields in the gap with the lossless eigenmode fields:

$$e_\mu^{\text{sim}}(\omega) = \frac{\int \mathbf{E}^{\text{sim}}(\mathbf{r},\omega)\cdot\mathbf{E}_\mu^* dV}{\int \mathbf{E}_\mu\cdot\mathbf{E}_\mu^* dV}, \quad (38)$$

where $\mathbf{E}^{\text{sim}}(\mathbf{r},\omega)$ is the field sampled from the simulation in the gap between the cube and the substrate, and V is the volume of the gap where the lossless eigenmodes are defined.

Based on the simulation results shown in Fig. 3, it is apparent that there are only two lossless eigenmodes that play a significant role when the cube is illuminated under normal incidence. The fundamental mode $e_{1,0}$ appears as expected. This mode is a bright mode, and is commonly used in fluorescence enhancement and other applications where a high quantum yield is desired [4].

An additional higher order mode $e_{1,2}$ also has a small peak near 430 nm. This mode may be called a "dark mode," since it exhibits nearly zero radiative loss. The appearance of this mode is surprising, since the integral in Eq. (32a) would require that the mode $e_{1,2}$ has zero coupling to the incident field when excited at normal incidence. It will be shown in Secs. IV B and IV C that the excitation of this mode can be explained by allowing for the eigenmodes of the system to be nonorthogonal

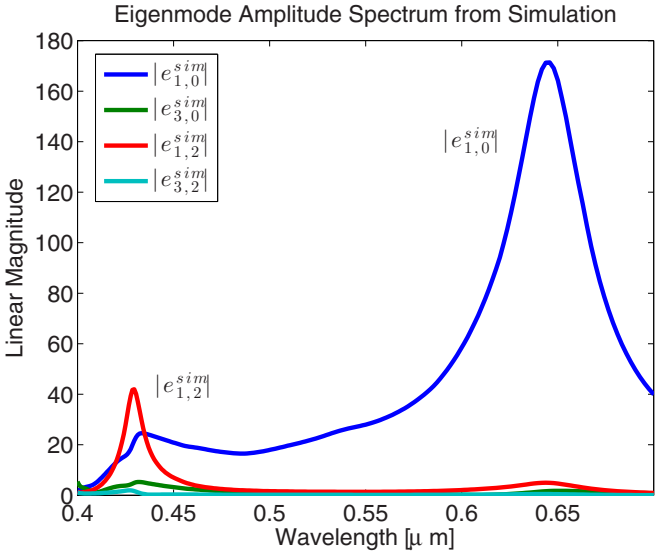

FIG. 3. (Color online) The eigenmode amplitude spectrum extracted from full-wave simulation of an 80 nm cube using Eq. (38). The fundamental, bright mode is $|e_{1,0}^{\text{sim}}(\omega)|$, while $|e_{1,2}(\omega)|$ is a higher order dark mode.

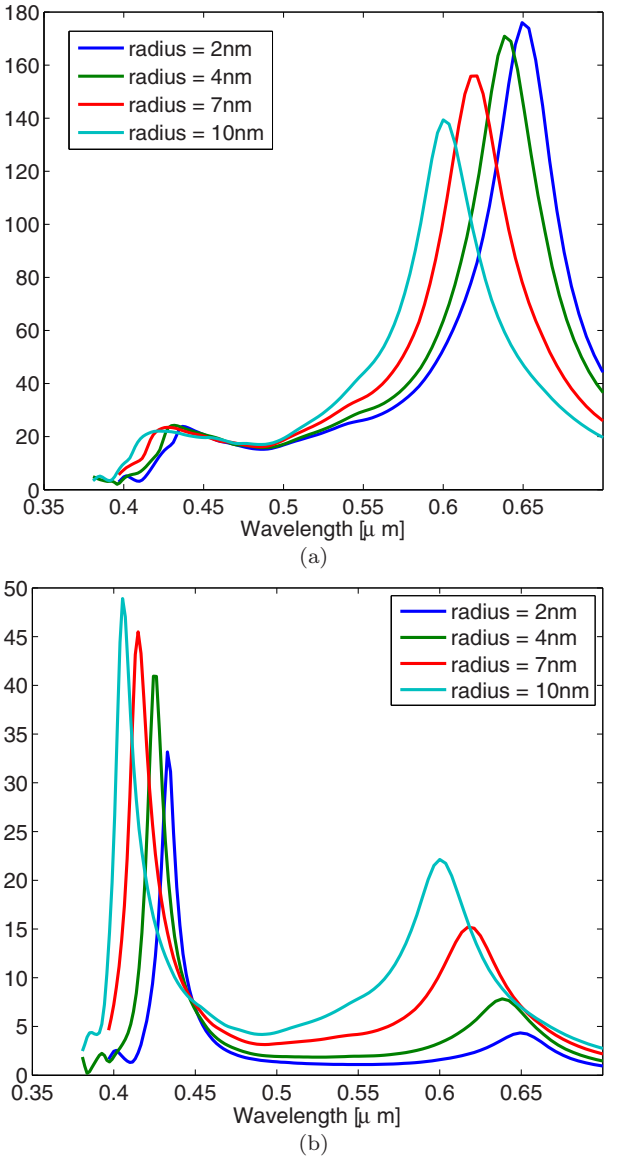

FIG. 4. (Color online) (a) The amplitude of the bright mode is plotted as the radius of curvature of the corners of the cube is varied. (b) The amplitude of the dark mode is plotted as the radius of curvature is varied. The resonance frequency of both modes shifts roughly linearly in wavelength as the radius of curvature is varied, and the coupling to the dark mode increases with increasing radius of curvature.

due to the radiative losses. A modal cross coupling between the bright and dark modes is also consistent with the strong amplitude transition of the bright mode at the dark mode resonance frequency, and the small peak in the dark mode at the bright mode resonance frequency (see Fig. 4). This modal cross coupling can be captured using the formalism developed in Sec. IV A by allowing the radiative loss matrix to have nonzero off-diagonal matrix elements, which will be demonstrated in Secs. IV B and IV C.

The quality factor and maximum excitation of the bright mode amplitude can be very accurately predicted using Eq. (32a). Unfortunately, the imaginary part of the surface impedance in Eq. (36) does not give the correct frequency

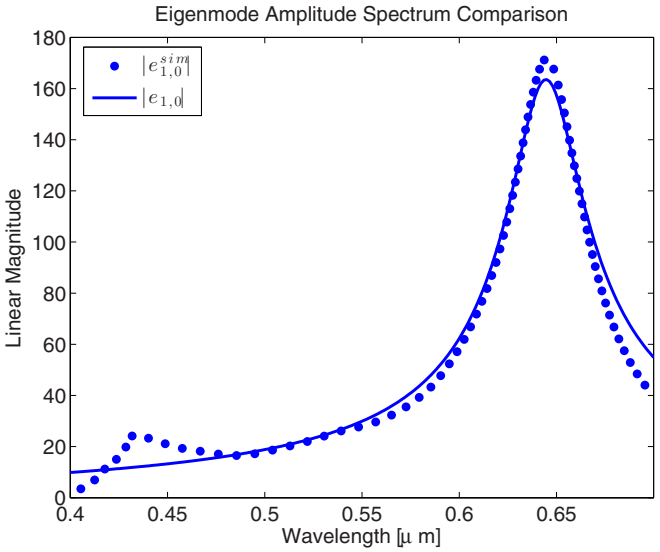

FIG. 5. (Color online) Comparison of the magnitude of the fundamental mode extracted from full-wave simulation, $|e^{\text{sim}}_{1,0}(\omega)|$, with the magnitude of the fundamental mode analytically computed from Eq. (32a), $|e_{1,0}(\omega)|$. A correction factor of 0.3 is included in the imaginary part of the impedance to accommodate the frequency shift.

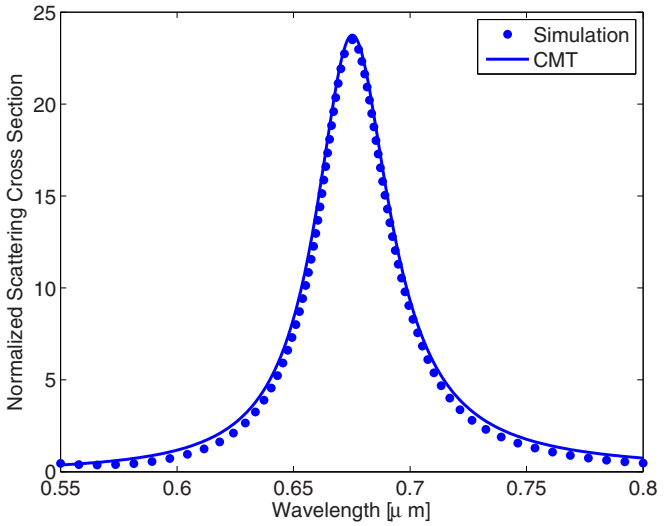

FIG. 6. (Color online) Normalized scattering cross section, defined by $\text{SCS} = P_{\text{scatt}}/W^2 I_{\text{inc}}$, where I_{inc} is the intensity of the normally incident beam.

shift for the fundamental mode. Some disagreement is to be expected since it doesn't take into account the finite size of the cube, the nonconstant distribution of the field on two of the sides, or the interactions between the various sides of the cube. However, good agreement with simulation is obtained if the imaginary part of the impedance given in Eq. (36) is multiplied by a constant factor of 0.3, as shown in Fig. 5. We note that this correction factor is dependent on the radius of curvature of the edges of the cube and the height of gap, not unlike the corrections used when computing the effective resonance wavelength of optical nanorod antennas [30].

In Fig. 4 we study the impact of the radius of curvature on the resonance frequency of the modes and the correction factor for the imaginary part of the surface impedance. Based on the simulation results in Fig. 4, as the radius of curvature increases, the resonance frequency of both the bright and dark modes increases while the excitation of the dark mode also increases. The effects of increasing the correction factor in the coupled-mode theory model are that the resonance frequency of each of the modes decreases, and the cross coupling between modes with nonzero surface integrals increases. For this reason, the finite radius of curvature cannot be modeled by only modifying the effective imaginary surface impedance, but the effective width of the cube should also be decreased as the radius of curvature is increased so that the resonance frequency is increased in a way that is consistent with Fig. 4. This idea of an effective cube width has also been used in both optical [14] and RF patch antenna theory [24] to account for the shift in resonance frequency of the modes from the ideal value computed by the dispersion relation. In this paper we choose to analyze cubes with a radius of curvature of 2 nm, where the effective width is identical with the width of the cube and the correction factor on the surface impedance is 0.3. A larger radius of curvature could be modeled by changing both the effective width of the cube and the imaginary surface impedance accordingly.

The eigenmode expansion formalism has also given an easy, intuitive approach to calculating various experimentally measurable parameters. As an example, we consider the total scattered power of the cube, which can be intuitively calculated from the radiative loss matrix. In the orthogonal case, the scattered power is given by

$$P_{\text{scatt}} = \frac{1}{2}\int_{\text{slots}} \text{Re}\{\mathbf{E}\times\mathbf{H}^*\}\cdot\mathbf{n}dS = \sum_{\mu}\text{Re}\left\{e_\mu h^*_\mu U_\mu P^{\text{rad}*}_\mu\right\}, \tag{39}$$

which gives excellent agreement with the scattered power found from the simulation results in Fig. 6.

B. Modal cross coupling due to radiation damping: surface impedance approach

In the nanocube system, and in lossy systems in general, the loss matrices are not diagonal, even though in this case the ohmic losses are well approximated by a diagonal matrix. The cross coupling in the radiation matrix can be seen by looking at the impedance-boundary form of $P^{\text{rad}}_{\mu\nu}$ and comparing with the eigenmode fields defined in Eq. (3). The overlap integral of the tangential components,

$$P^{\text{rad}}_{\mu\nu}(\omega) = -\frac{Y_g(\omega)}{2}\int(\mathbf{E}^*_\mu\times\mathbf{n})\cdot(\mathbf{E}_\nu\times\mathbf{n})dS, \tag{40}$$

will not always be zero for different modes. Using this form for the radiative loss matrix, together with Eqs. (22) and (18), the mode amplitude equations become

$$h_\mu = (\omega_\mu/\omega - jP^\Omega_\mu/\omega)e_\mu \tag{41}$$

$$\sum_\nu\left[j\left(\omega-\frac{\omega_\mu}{\omega}\left(\omega_\mu - jP^\Omega_\mu\right)\right)\delta_{\mu\nu}+P^{\text{rad}}_{\mu\nu}\right]e_\nu = -\int(\mathbf{E}^*_\mu\times\mathbf{H}_0)\cdot\mathbf{n}dS/U_\mu. \tag{42}$$

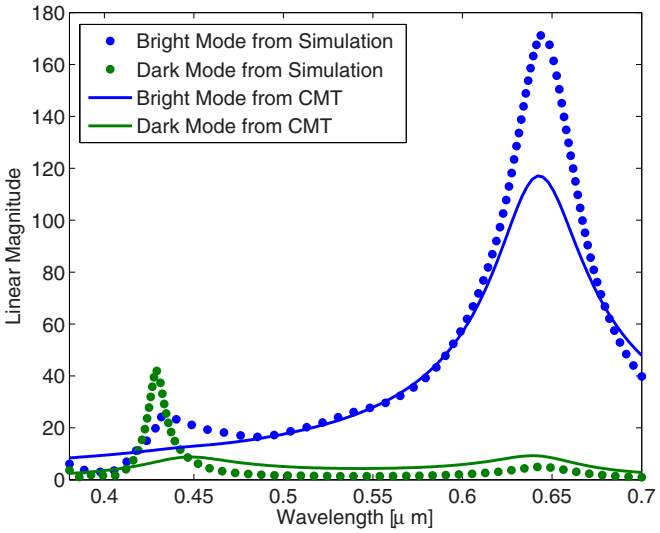

FIG. 7. (Color online) Magnitude of the main bright mode $e_{1,0}$ and the dark mode $e_{1,2}$ found analytically using Eqs. (41) and (42). The magnitudes of the corresponding modes were extracted from simulation and are shown in the dotted lines.

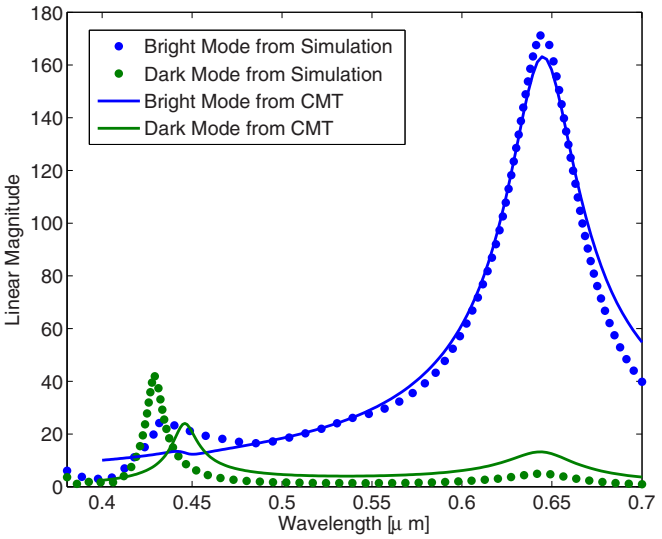

FIG. 8. (Color online) Magnitude of the main bright mode and the dark mode using an analytically evaluated radiative loss matrix, and compared to full-wave simulation results. A correction factor of 0.29 was included in the imaginary part of the radiation impedance to accommodate the resonance frequency shift.

The left-hand side of the electric mode amplitude equation forms a matrix that may be inverted to solve the system. The array factor is included as outlined in Sec. IV A. With these assumptions, and using the correction factor on the surface impedance of 0.3 that was determined in IV A, the model gives the results shown in Fig. 7.

Although this is a crude approach to deterring the exact elements of the radiative loss matrix, it does give an explanation for why the E_{21} eigenmode is excited. For many eigenmodes of the structure, the surface integral of the tangential component of the fields is zero across the gap for the lossless eigenmode fields. However, for the modes E_{10} and E_{12}, the surface overlap integral is large and nonzero on two opposite sides of the cube. Therefore these modes become coupled through the surface admittance of the gap.

Since the surface impedance given in Eq. (36) comes from an expression that assumes an infinitely wide slot with constant electric field, using this approximation in Eq. (40) greatly overestimates the radiative losses due to slots that do not have a constant electric field. The result is that both the bright mode and the dark mode appear to be much more damped than is seen in simulation.

C. Modal cross-coupling due to radiation damping: Fourier method

If the impedance assumption is not made, then the radiative loss matrix is given by

$$P^{\mathrm{rad}}_{\mu\nu}(\omega) = \frac{1}{2}\int (\mathbf{E}^*_\mu \times \mathbf{H}_\nu)\cdot \mathbf{n} dS, \tag{43}$$

where $\mathbf{E}_\mu$ is the exact eigenmode field, and the tangential component of $\mathbf{H}_\nu$ on the surface is given by the Fourier method presented in the Appendix. These matrix elements will again be a function of frequency. The real part of the radiative loss matrix may be determined by this method, but the imaginary part is shown in the appendix to not converge. Therefore the imaginary part will remain approximated by a surface impedance as it was in Sec. IV C.

In this formulation of the problem, the system solution is given by the linear system

$$h_\mu = (\omega_\mu/\omega - jP^\Omega_\mu/\omega)e_\mu \tag{44}$$

$$\sum_\nu \left[j\left(\omega - \frac{\omega_\mu}{\omega}\left(\omega_\mu - jP^\Omega_\mu\right)\right)\delta_{\mu\nu} + \left(\left(\omega_\mu - jP^\Omega_\mu\right)/\omega\right)P^{\mathrm{rad}}_{\mu\nu}\right] e_\nu = -\int (\mathbf{E}^*_\mu \times \mathbf{H}_0)\cdot \mathbf{n} dS/U_\mu, \tag{45}$$

where the matrix on the left hand side must be inverted to solve the system. Solving this system using eigenmodes with (m,n) ranging from (0,0) to (2,2) gives excellent agreement with simulation results shown in Fig. 8.

The solution to this equation works very well compared to the simulation results for the fundamental mode, and it reproduces the main features of the dark mode. The resonance frequency does appear to be shifted for the dark mode, and this disagreement is likely because the imaginary part of the radiation matrix is still used to compute the radiation loss matrix, which determines the resonance frequency shift of the modes. The imaginary part assumes that the mode profile is constant across the gap, and this approximation is worse for higher order modes. Therefore we do not expect as good agreement for the higher order modes, but it qualitatively reproduces their behavior and cross coupling to the fundamental mode.

V. CONCLUSION

We have presented a semianalytic perturbed eigenmode approach to solving for the fields in the gap of a film-coupled nanocube. The approach is able to accurately predict simulation results, predict scattering spectra, and provide insight into why specific modes become coupled, despite only approximately accounting for the cross coupling between modes due to losses and the resonance frequency shift due to reactive power. Full-wave simulations will always be needed to verify analytical efforts, but the overall approach provides powerful insight into the field interactions in the gap. Using this eigenmode approach ultimately allows an effective Green's function of the cube to be constructed, which can then be further used to predict coupling due to arbitrary far-field sources or dipolar sources within the gap.

ACKNOWLEDGMENT

This work was supported by the Air Force Office of Scientific Research (AFOSR, Grant No. FA9550-12-1-0491).

APPENDIX A: OHMIC LOSSES

Unlike the radiative loss matrix, where a closed-form expression for the exact, lossy magnetic field is unknown in the slots, the electric field of the lossy eigenmodes can be found analytically on the bottom of the cube and top of the film using Eq. (3) and allowing k_x to be the value found by solving the dispersion relation in Eq. (4) using a complex permittivity. Then it can be seen by inspection of Eq. (3) that this overlap surface integral is only nonzero for $\mu = \nu$, and therefore the modes do not couple to each other due to Ohmic losses. This result can be used to simplify Eq. (18) by requiring that the Ohmic loss matrix in Eq. (19) is purely diagonal,

$$j\omega h_\mu U_\mu - j\omega_\mu e_\mu U_\mu + e_\mu P_\mu^\Omega = \frac{1}{2}\int \mathbf{H}_\mu^* \cdot \mathbf{J}_m dV, \quad \text{(A1)}$$

where $P_\mu^\Omega = \frac{1}{2U_\mu}\int(\tilde{\mathbf{E}}_\mu \times \mathbf{H}_\mu^*)\cdot \mathbf{n} dS$ and is given by

$$P_{\mu(m,n)}^\Omega = \frac{2cW^2}{\pi^2 h(m^2+n^2)}\mathrm{Re}\{-ik_{xmn}\sin(k_{xmn}h/2)\omega_{mn}/c\}. \quad \text{(A2)}$$

In this equation, the single index μ has been given an arbitrary mapping to a double index mn using the notation $\mu(m,n)$.

APPENDIX B: FOURIER METHOD FOR EVALUATING COUPLING COEFFICIENTS

To find the radiative losses due to the gap between the cube and the substrate, radiative boundary conditions need to be taken into account to fix the integral of the Poynting vector over the gap. To do this, we apply a Fourier transform method, following the approach commonly used to examine radiation patterns by aperture antennas [24]. We are considering matrix elements of the form

$$P_{\mu\nu}^{\mathrm{rad}}(\omega) = \frac{1}{2}\int(\mathbf{E}_\mu^* \times \mathbf{H}_\nu)\cdot \mathbf{n} dS, \quad \text{(B1)}$$

where the surface integral is applied all four sides of the cube-substrate gap. Even though the lossless eigenmode fields $\mathbf{E}_\mu$ and $\mathbf{H}_\mu$ are not functions of frequency, the radiation loss is a function of frequency, and therefore the overlap integral of the lossy eigenmode fields may also be a function of frequency.

The heart of the Fourier method is the assumption that the electric field in the slot is equal to the lossless eigenmode field. The method then uses Fourier transforms to deter the magnetic field in the slot the given electric field profile. However, because this method assumes that the electric field is equal to the lossless eigenmode field, it will only be valid as long as that approximation holds.

The subscripts for the modes will temporarily be ignored in order to outline the method and then will be reintroduced later. According to Parseval's theorem, the surface integral of the Poynting vector over any particular slot can be rewritten as

$$\iint_{A_1}(\mathbf{E}\times\mathbf{H}^*)\cdot\mathbf{n}dS = \frac{1}{8\pi^2}\iint_{-\infty}^{\infty}(\mathcal{E}\times\mathcal{H}^*)\cdot\mathbf{n}dS_{\mathbf{k}}, \quad \text{(B2)}$$

where $\mathcal{E}_\mu$ and $\mathcal{H}$ are the spatially Fourier transformed fields across one of the apertures, and $dS_{\mathbf{k}}$ is an area element in the k space of the tangential coordinates to the aperture. To make the formulation a bit more clear, let $\mathbf{r} = \{x,y,z\}$ be arranged such that the z coordinate be defined as normal to the aperture, the x coordinate as normal to the metal film, the y coordinate tangential to the aperture, and the origin lie in the center of the aperture. Then $\mathcal{E}$ and $\mathcal{H}$ are given by

$$\mathcal{E}(k_x,k_y,0) = \iint \mathbf{E}(x,y,0)e^{i(k_x x+k_y y)}dxdy \quad \text{(B3)}$$

$$\mathcal{H}(k_x,k_y,0) = \iint \mathbf{H}(x,y,0)e^{i(k_x x+k_y y)}dxdy. \quad \text{(B4)}$$

Notice that these are only transformed into Fourier space along the aperture dimensions, but the function is dependent on real space in the third dimension. The spatially Fourier transformed Ampere's law requires that the total magnetic field be related to the total electric field by

$$\mathcal{H} = \frac{1}{kZ_0}(\mathbf{k}\times\mathcal{E}). \quad \text{(B5)}$$

The Fourier transformed Gauss's law also requires that

$$\mathbf{k}\cdot\mathcal{E} = 0 \quad \text{(B6)}$$

$$\mathcal{E}_z = -\frac{k_x}{k_z}\mathcal{E}_x - \frac{k_y}{k_z}\mathcal{E}_y. \quad \text{(B7)}$$

Therefore, if the total tangential electric field is known at the aperture, then the normal component of the electric field and all three components of the magnetic field can be determined. It was shown in previous work that, for small gap heights, $\frac{|E_y|}{|E_x|} = \frac{|k_y|}{|k_x|}\tan(k_x h/2) \approx 0$, where h is the height of the gap. The electric field is therefore dominated by the x component when the gap size is sufficiently small [14]. Applying these approximations, the Fourier transformed field components become

$$\mathcal{E}_x = \iint_{A_1} E_x(x,y,0)e^{i(k_x x+k_y y)}dxdy \quad \text{(B8)}$$

$$\mathcal{E}_y = 0 \quad \text{(B9)}$$

$$\mathcal{E}_z = -\frac{k_x}{k_z}\mathcal{E}_x \quad \text{(B10)}$$

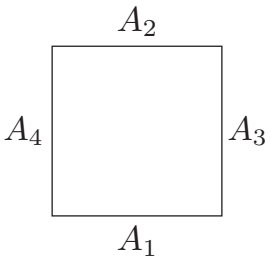

FIG. 9. Labeling convention for sides of the cube.

$$\mathcal{H}_x = 0 \tag{B11}$$

$$\mathcal{H}_y = \frac{1}{kZ_0}\left(\frac{k^2 - k_y^2}{k_z}\right)\mathcal{E}_x. \tag{B12}$$

These components could be used to evaluate Eq. (B2). However, since the method outlined here is only set up to calculate the integral over single planar surface, a correction factor (i.e., array factor) needs to be included to take the interaction of the various sides of the cube into account. To take the array factor into account, we consider sides of the cube in pairs.

$$P_{\mu\nu}^{\text{rad}} = \frac{1}{2}\iint_{A_1\cup A_2\cup A_3\cup A_4}(\mathbf{E}\times\mathbf{H}^*)\cdot\mathbf{n}dS \tag{B13}$$

$$= \frac{1}{2}\iint_{A_1\cup A_2}(\mathbf{E}\times\mathbf{H}^*)\cdot\mathbf{n}dS + \frac{1}{2}\iint_{A_3\cup A_4}(\mathbf{E}\times\mathbf{H}^*)\cdot\mathbf{n}dS, \tag{B14}$$

where A_1 and A_2 are two slots on opposite sides of the cube, and A_3 and A_4 are the other pair of parallel slots, as illustrated in Fig. 9.

The total power radiated out of two oppositely facing apertures is then written as

$$\iint_{A_1\cup A_2}(\mathbf{E}\times\mathbf{H}^*)\cdot\mathbf{n}dS \tag{B15}$$

$$= \frac{1}{8\pi^2 Z_0}\iint_{-\infty}^{\infty}|AF|^2\left(\frac{1-(k_y/k)^2}{\sqrt{1-(k_x/k)^2-(k_y/k)^2}}\right)\times|\mathcal{E}_x|^2 dk_x dk_y, \tag{B16}$$

where AF is the array factor, and $k_z = k\sqrt{1-(k_x/k)^2-(k_y/k)^2}$ has been used. Only the real part of the surface integral term should be modified by the array factor, because the imaginary part represents evanescent fields that do not interact over long distances. The array factor itself is a function of frequency and depends on the direction of radiation under consideration. However, for smaller cubes, the array factor is well approximated as zero if the electric field of the eigenmode is even across two oppositely facing apertures, and two if the electric field of the eigenmode is odd across two oppositely facing apertures.

Now, we consider matrix elements of the form

$$\iint_{A_1\cup A_2}(\mathbf{E}_\mu\times\mathbf{H}_\nu^*)\cdot\mathbf{n}dS \tag{B17}$$

$$= \frac{1}{8\pi^2 Z_0}\iint_{-\infty}^{\infty}|AF|^2\left(\frac{1-(k_y/k)^2}{(k_z/k)}\right)\mathcal{E}_\mu\mathcal{E}_\nu^* dk_x dk_y, \tag{B18}$$

where $\mathcal{E}_\mu$ is the Fourier transform of the x component of the electric field of the μth mode.

The Fourier transformed field can be found analytically to be

$$\mathcal{E}_\nu = hW\,\text{sinc}(k_x h/2)\sin(k_y W/2)\frac{k_y W/2}{(\nu\pi/2)^2-(k_y W/2)^2} \quad (\text{even } \nu) \tag{B19}$$

$$\mathcal{E}_\nu = hW\,\text{sinc}(k_x h/2)\cos(k_y W/2)\frac{k_y W/2}{(\nu\pi/2)^2-(k_y W/2)^2} \quad (\text{odd } \nu). \tag{B20}$$

Compiling these equations together will give the solution for the radiated power. The difficulty here, however, is that the imaginary part diverges. The real part is given by integrating over the open disk $D_0(k) = \{(k_x,k_y)|\sqrt{k_x^2+k_y^2} < k^2\}$. However, the imaginary part of the integral involves integrating over the rest of k space, and the integrand goes as $1/k_y$ for large k_y, so the k_y part of the integral will not converge.

In order to fix the imaginary component, one must either obtain a better approximation for the fields in the slot, or else resort to an approximation. Here we resort again to the imaginary part of the surface admittance for an open-ended parallel-plate waveguide.

$$\text{Im}\{P_{\mu\nu}^{\text{rad}}(\omega)\} = -\frac{\text{Im}\{Y_g(\omega)\}}{2}\int(\mathbf{E}_\mu^*\times\mathbf{n})\cdot(\mathbf{E}_\nu\times\mathbf{n})dS, \tag{B21}$$

where $Y_g(\omega)$ is given in Eq. (36).

[1] G. Lévêque and O. J. Martin, Opt. Lett. **31**, 2750 (2006).
[2] B. Sturman, E. Podivilov, and M. Gorkunov, Phys. Rev. B **87**, 115406 (2013).
[3] P. Anger, P. Bharadwaj, and L. Novotny, Phys. Rev. Lett. **96**, 113002 (2006).
[4] M. H. Mikkelsen, A. Rose, T. B. Hoang, F. McGuire, J. J. Mock, C. Ciraci, and D. R. Smith, in *CLEO: 2014* (Optical Society of America, San Jose, CA, 2014), p. FW1C.3.
[5] S. Mukherjee, F. Libisch, N. Large, O. Neumann, L. V. Brown, J. Cheng, J. B. Lassiter, E. A. Carter, P. Nordlander, and N. J. Halas, Nano Lett. **13**, 240 (2013).

[6] C. Argyropoulos, C. Ciraci, and D. R. Smith, Appl. Phys. Lett. **104**, 063108 (2014).
[7] D. J. Bergman and M. I. Stockman, Phys. Rev. Lett. **90**, 027402 (2003).
[8] W. Wenseleers, F. Stellacci, T. Meyer-Friedrichsen, T. Mangel, C. A. Bauer, S. J. K. Pond, S. R. Marder, and J. W. Perry, J. Phys. Chem. B **106**, 6853 (2002).
[9] E. Poutrina, C. Ciracì, D. J. Gauthier, and D. R. Smith, Opt. Express **20**, 11005 (2012).
[10] W. R. Holland and D. G. Hall, Phys. Rev. Lett. **52**, 1041 (1984).
[11] A. Aubry, D. Y. Lei, S. A. Maier, and J. B. Pendry, ACS Nano **5**, 3293 (2011).
[12] J. J. Mock, R. T. Hill, A. Degiron, S. Zauscher, A. Chilkoti, and D. R. Smith, Nano Lett. **8**, 2245 (2008).
[13] G. Lévêque and O. J. F. Martin, Opt. Express **14**, 9971 (2006).
[14] C. Ciraci, J. Britt Lassiter, A. Moreau, and D. R. Smith, J. Appl. Phys. **114**, 163108 (2013).
[15] G. Veronis and S. Fan, Opt. Lett. **30**, 3359 (2005).
[16] A. Moreau, C. Cirac, J. J. Mock, R. T. Hill, Q. Wang, B. J. Wiley, A. Chilkoti, and D. R. Smith, Nature (London) **492**, 86 (2012).
[17] J. B. Lassiter, F. McGuire, J. J. Mock, C. Cirac, R. T. Hill, B. J. Wiley, A. Chilkoti, and D. R. Smith, Nano Lett. **13**, 5866 (2013).
[18] S. Fan, W. Suh, and J. D. Joannopoulos, J. Opt. Soc. Am. A **20**, 569 (2003).
[19] L. Verslegers, Z. Yu, P. B. Catrysse, and S. Fan, J. Opt. Soc. Am. B **27**, 1947 (2010).
[20] H. Haus, *Waves and Fields in Optoelectronics*, Prentice-Hall Series in Solid State Physical Electronics (Prentice Hall, Englewood Cliffs, NJ, 1984).
[21] Q. Bai, M. Perrin, C. Sauvan, J.-P. Hugonin, and P. Lalanne, Opt. Express **21**, 27371 (2013).
[22] Y. Zeng, D. A. R. Dalvit, J. O'Hara, and S. A. Trugman, Phys. Rev. B **85**, 125107 (2012).
[23] A. Raman and S. Fan, Phys. Rev. Lett. **104**, 087401 (2010).
[24] C. A. Balanis, *Antenna Theory: Analysis and Design* (John Wiley and Sons, Hoboken, NJ, 2005).
[25] R. E. Collin, *Field Theory of Guided Waves*, IEEE/OUP Series on Electromagnetic Wave Theory (IEEE Press, New York, 1991), published under the sponsorship of the IEEE Antennas and Propagation Society.
[26] J. Yang, C. Sauvan, A. Jouanin, S. Collin, J.-L. Pelouard, and P. Lalanne, Opt. Express **20**, 16880 (2012).
[27] F. Wang and Y. R. Shen, Phys. Rev. Lett. **97**, 206806 (2006).
[28] S. Schelkunoff, Bell Syst. Tech. J. **15**, 92 (1936).
[29] P. B. Johnson and R. W. Christy, Phys. Rev. B **6**, 4370 (1972).
[30] L. Novotny, Phys. Rev. Lett. **98**, 266802 (2007).